THE OFFICIAL MAGAZINE OF THE OCEANOGRAPHY SOCIETY

Oceanography

CITATION

Matano, R.P., and E.D. Palma. 2018. Seasonal variability of the oceanic circulation in the Gulf of San Jorge, Argentina. *Oceanography* 31(4):16–24, https://doi.org/10.5670/oceanog.2018.402.

DOI

https://doi.org/10.5670/oceanog.2018.402

Seasonal Variability of the Oceanic Circulation in the Gulf of San Jorge, Argentina

By Ricardo P. Matano and Elbio D. Palma

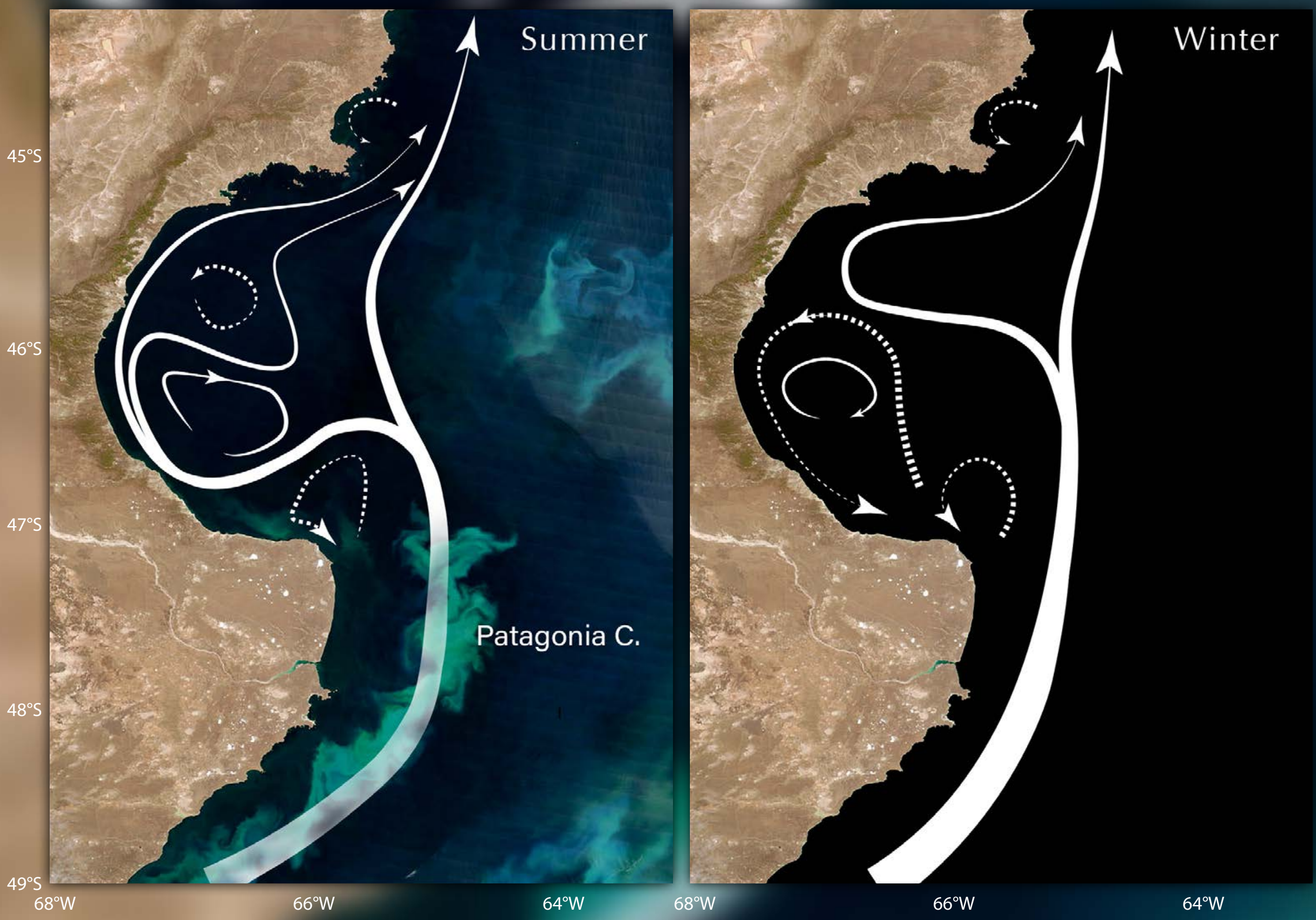

Schematic representation of the depth-averaged Gulf of San Jorge circulation during summer and winter. Solid lines indicate cyclonic circulation, dashed lines indicate anticyclonic circulation.

ABSTRACT. This study uses a high-resolution model to characterize the seasonal variability of the oceanic circulation in the Gulf of San Jorge (Argentina). The time mean circulation is dominated by a cyclonic gyre bounded by a relatively strong coastal current and, on its offshore side, by the Patagonia Current. The gulf circulation varies significantly with season. Tidal mixing during the summer months generates baroclinic pressure gradients that allow development of a cyclonic gyre in the southern region. During winter, erosion of density gradients weakens the cyclonic tendency and a large anticyclonic gyre develops in the southern region. Atmospheric heat fluxes regulate the transition between summer and winter circulation patterns. Analysis of process-oriented experiments indicates that summer circulation is mainly driven by the interaction between tides and stratification while winter circulation is mainly driven by wind forcing. The mass exchanges between the gulf and the open shelf peak during the summer due to a larger onshore penetration of the Patagonia Current. During winter, these exchanges are very weak and remain largely confined to the northern portion of the gulf.

INTRODUCTION

The Gulf of San Jorge (GSJ) is the largest gulf of the Patagonian Shelf, the southernmost portion of the eastern shelf of South America, and one of the most productive regions of the world ocean (Costanza et al., 1997; Figure 1a). The GSJ hosts Argentina's second largest oil and natural gas reservoirs (Silwan, 2001) and harbors some of its most valuable fishery stocks, including hake, Patagonian scallops, king crabs, and shrimps (Bogazzi et al., 2005; Glembocki et al., 2015). The gulf ecosystem and its regional economic activities depend on the characteristics of the local oceanic circulation, which are largely unknown. In fact, with the exception of a few highly specific regional studies, there are no descriptions of the GSJ circulation or its connection to the Patagonian Shelf. This is a matter of concern because the steady increases in oil-related activities and commercial fishing pose great environmental risks to local marine ecosystems, which cannot be evaluated without a proper understanding of the characteristics of regional oceanic circulation. To address this deficit, we used a suite of high-resolution numerical experiments to characterize the main features of GSJ circulation, its seasonal variations, and its exchanges with the neighboring shelf.

BACKGROUND

The GSJ extends from 47°S (Cape Tres Puntas) to 45°S (Cape Dos Bahías), encompassing an approximate area of 40,000 km^2 (Figure 1a). The most noteworthy features of the bottom topography of this relatively shallow gulf are the Central Basin, a 100 m depression located at its center, and South Bank, a shallow bank that separates the southern portion of the gulf from the open shelf (Figure 1b). The thermohaline characteristics of the gulf's waters are controlled by atmospheric heat and freshwater fluxes and by onshore intrusions of the Patagonia Current. There are no significant freshwater discharges into the GSJ. Local wind forcing is dominated by strong and persistent westerlies. The relatively small seasonal variations in the local winds are characterized by intensification during late fall, weakening at the end of winter, and strengthening at the end of spring (Palma et al., 2004b; Combes and Matano, 2014, Figure 1a). The tidal cycle is dominated by the M_2 semidiurnal component, which enters the Patagonian Shelf through its southern boundary and propagates toward the north. Tidal amplitudes within the GSJ reach a maximum of 2 m near Comodoro Rivadavia (Figure 1b). The speed of the semidiurnal tidal currents peaks near Cape Tres Puntas. The interaction between tidal currents and bottom topography near South Bank generates the third largest tidal dissipation center of the entire Patagonian Shelf (Palma et al., 2004a).

There are few descriptions of the GSJ circulation (Palma et al., 2004a; Tonini et al., 2006; Glembocki et al., 2015; Krock et al., 2015). Krock et al. (2015) reported the intrusion of low-salinity waters from the Patagonia Current—a shelf current formed by discharges from the Magellan Straits (Brandhorst and Castello, 1971; Palma and Matano, 2012)—at intermediate depths, and the existence of an intense thermohaline front at the southern end of the gulf. Using satellite sea surface temperature and chlorophyll *a* data, Glembocki et al. (2015) identified three thermal fronts, the southernmost of which strengthens during winter. They related this strengthening to the effects of tidal mixing, while development of the northernmost front was proposed to be due to vertical stratification during spring and summer. Glembocki et al. (2015) identified another front over South Bank, which begins developing during spring and reaches its maximum extent during summer. There is no further information on the characteristics of these fronts or the underlying dynamics of their variability.

Previous modeling studies of GSJ circulation focused on the impact of tidal and wind forcing on the gulf mean circulation. Tonini et al. (2006) identified a tidal dissipation center over South Bank and showed the development of a cyclonic gyre in the northern half of the gulf and an anticyclonic gyre in the southern half. Their model also revealed the development of a wind-driven upwelling center along the south and southwest coasts and a downwelling center along the northern coast. Models with a larger (shelf-wide) domain but lower spatial resolution show similar features (Glorioso and Flather, 1995; Palma et al., 2004a).

The scant information about the kinematics of the gulf circulation makes characterization of its dynamics difficult, particularly identification of the role of local and remote forcing in the shaping of the gulf's water mass characteristics. The lack of in situ observations is compounded by the deficiencies of previous numerical studies, which are too idealized (Tonini et al., 2006) or lack the proper spatial resolution to address local features (Palma et al., 2008; Combes and Matano, 2014). We address some of these deficiencies by analyzing a suite of high-resolution numerical experiments specifically designed to characterize the kinematics and dynamics of the GSJ circulation and its seasonal variability. The following section offers a brief technical description of the model configuration, and subsequent sections discuss the model results. The discussion will be focused on the time mean circulation, its seasonal variability, and the mass exchanges between the GSJ and the open shelf.

MODEL DESCRIPTION

The numerical model used in this study is based on the Regional Ocean Modeling System (ROMS_AGRIF; Debreu et al., 2012). In the vertical, the model's primitive equations are discretized over variable topography using stretched terrain-following coordinates. The stretched coordinates allow increased resolution in areas of interest, such as surface and bottom boundary layers. In the horizontal, the primitive equations are evaluated using orthogonal curvilinear coordinates on a staggered Arakawa C-grid. Vertical mixing is parameterized with a K-Profile Parameterization (KPP) scheme (Large et al., 1994). The model domain extends from 58°S to 38°S and from 69°W to 54°W with 1/24° horizontal resolution. In the vertical, the model equations are discretized into 40 sigma levels, with higher vertical resolution at the top and bottom layers. The bathymetry is based on digitized nautical charts (Figure 1a). At the model's open boundaries we employ radiation and advection conditions (Marchesiello et al., 2001). There, we specify the amplitudes and phases of the M_2 tide, which are interpolated from a global TPX06 tidal model (Egbert et al., 1994). At these boundaries we also specify the climatological values of temperature, salinity, and velocity fields extracted from the Southern Hemisphere model of Combes and Matano (2014). At the surface we force the model with the mean climatological wind stress derived from

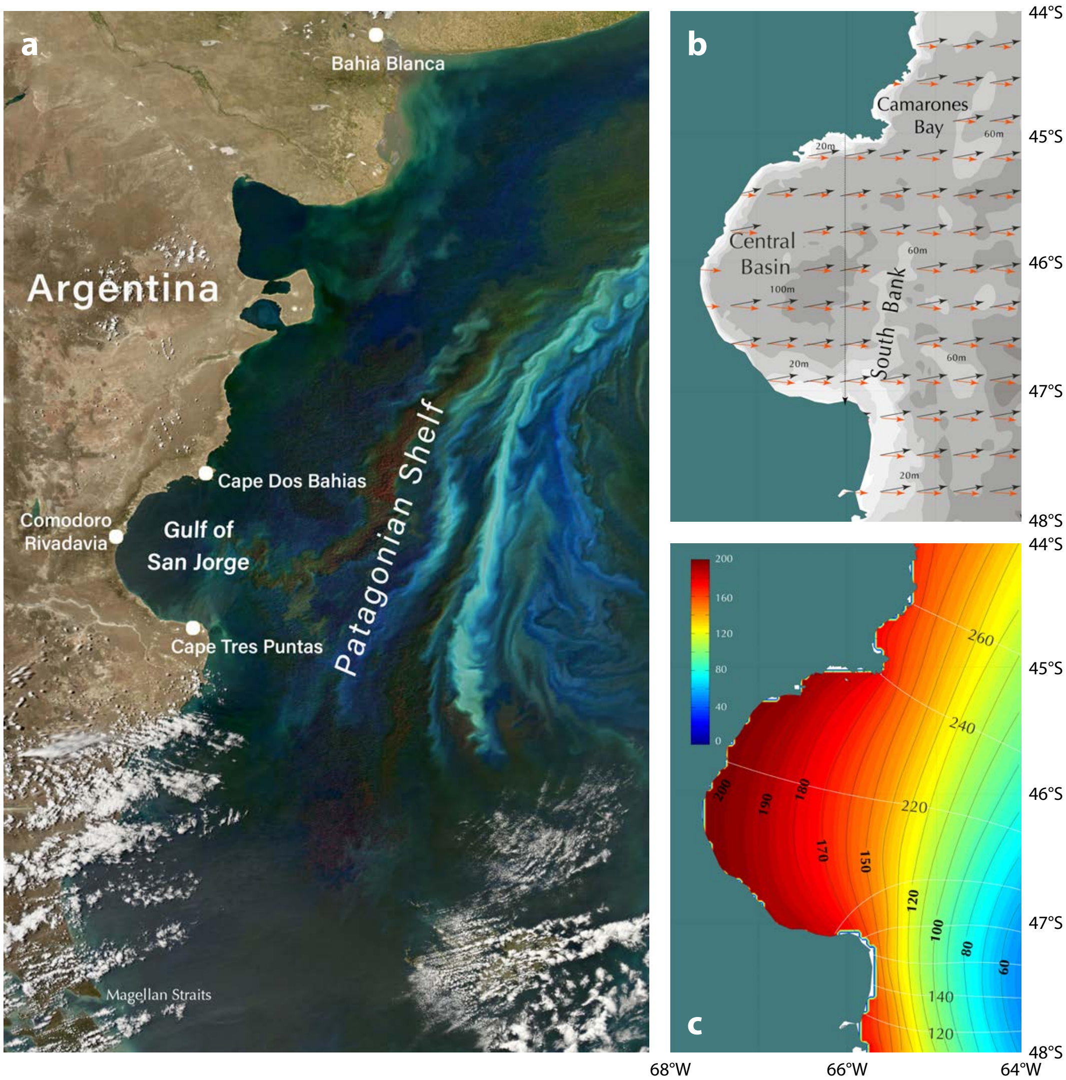

FIGURE 1. (a) MODIS chlorophyll image of the Patagonian shelf. (b) Bottom topography of the Gulf of San Jorge. The arrows represent the wind stress field during winter (black) and summer (red). The dotted black line indicates the location where mass exchanges are calculated. (c) Amplitudes (color) and phases (white contours) of the M_2 tide. Amplitude values are in centimeters.

the 1999–2012 Quikscat-ASCAT climatology. Heat and freshwater fluxes are computed as per Barnier (1998).

RESULTS

The dual objectives of the present analysis are to characterize the GSJ circulation and to identify its drivers. To this end, we first conducted a suite of process-oriented experiments—referred to as NONSTRAT—that are initialized with constant values of temperature and salinity and forced with different combinations of wind stress and tides. These experiments are used to understand the role of bottom topography, wind stress forcing, and tides in generating the GSJ circulation. A second experiment, STRAT, which is our most realistic representation of the local conditions, characterizes the actual circulation. STRAT is initialized with climatological profiles of temperature and salinity from observational data sets (Conkright et al., 2002) and forced with the atmospheric fluxes described in the previous section. Both sets of experiments are spun up to dynamic equilibrium and run prognostically for a five-year period.

NONSTRAT

This set includes three experiments: the first is forced with winds only, the second with tides only, and the third with both tides and winds. There is no heat or freshwater forcing; tides are the only open boundary forcing. Thus, NONSTRAT represents the circulation patterns generated in a gulf of constant density and variable bottom topography that is under the influence of wind and/or tidal forcing. The first three panels of Figure 2 (a, b, and c) show the stream function (color) and the residual depth-mean velocities (vectors) of this experimental suite. The circulation in the winds-only experiment shows a double gyre structure, with a larger anticyclone in the south and a smaller cyclone in the north (Figure 2a). This structure reflects the influence of open shelf circulation and local bottom topography. To understand how bottom topography leads to the formation of a double gyre structure, consider the steady state vorticity balance of a linear, barotropic, wind driven flow in a small basin (large Rossby radius),

$$curl_z\left(\frac{\vec{\tau}^{bottom}}{\rho_o D}\right) = curl_z\left(\frac{\vec{\tau}^{wind}}{\rho_o D}\right),$$

where τ^{bottom} and τ^{wind} represent the bottom stress and wind stress, ρ_0 the density, and D the basin depth. This simple balance states that in the steady state, the vorticity imparted by the wind should be dissipated by bottom friction. If the bottom stress is parameterized with a linear drag law, then

$$curl_z\left(\frac{\vec{\tau}^{bottom}}{\rho_0\ D}\right) = C_D\ \zeta,$$

where $\zeta = \frac{\partial v_{da}}{\partial x} - \frac{\partial u_{da}}{\partial y}$ is the vorticity of

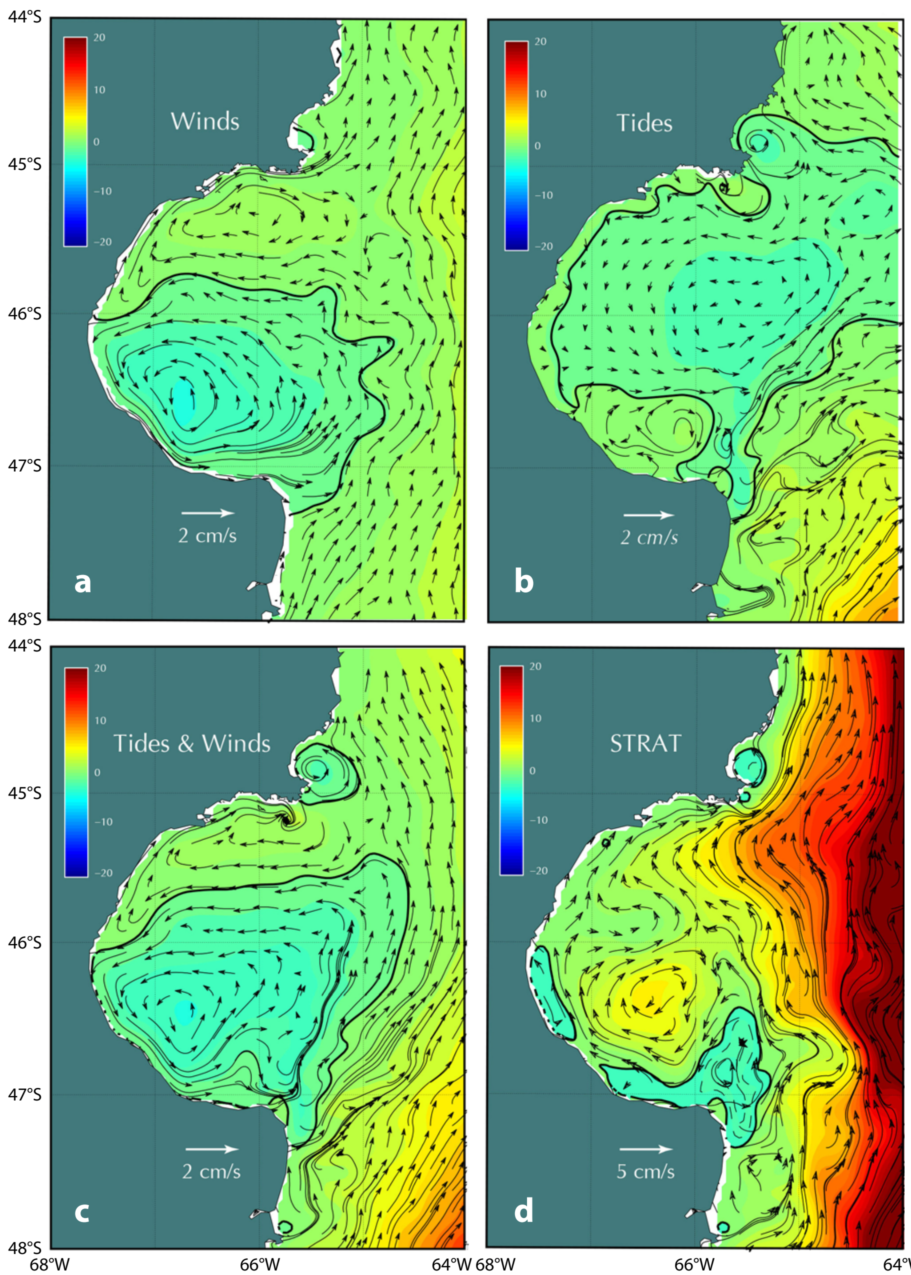

FIGURE 2. Annual mean stream function (colors in centi-Sv, or cSv: 1 cSv = 1 × 10^4 m^3 s^{-1}) and residual depth-mean velocity vectors from a suite of process-oriented experiments called NONSTRAT: (a) tidal forcing only, (b) wind forcing, and (c) tidal and wind forcing. (d) Annual mean stream function and residual depth-mean velocity vectors from the stratified experiment (STRAT). Thick black lines indicate the zero contour.

the depth-averaged flow, and C_D is a constant. It follows that

$$\zeta = \frac{1}{C_d} curl(\frac{\vec{\tau}^{wind}}{\rho_o D}) =$$

$$\frac{curl\left(\vec{\tau}^{wind}\right)}{C_d \rho_o D} + \frac{\vec{\tau}^{wind} \times \nabla D}{C_d \rho_o D^2}.$$

If $\vec{\tau}^{wind}$ = constant, the curl of the wind is zero, and vorticity generation occurs only if $\vec{\tau}^{wind}$ and ∇D are not parallel. In the GSJ region, the wind is predominantly westward, in which case the previous equation reduces to:

$$\zeta = \frac{1}{C_d \rho_o D^2} \tau_x^w \frac{\partial D}{\partial y}.$$

For the particular geometry and bathymetry of the GSJ, the meridional topographic gradient is negative in the northern half of the gulf and positive in the southern portion. It follows, therefore, that the wind injects positive vorticity, thus generating anticyclonic/anticlockwise circulation in the southern region and negative vorticity with cyclonic/clockwise circulation in the northern region (Figure 2a).

Residual circulation in the tides-only experiment is established by the nonlinear interaction between the oscillating tide and the bottom topography, which produces an elongated anticyclonic gyre centered over South Bank (Figure 2b). The nonlinear rectification of a tidal wave generates anticyclonic residual flows over banks and cyclonic residual flows over depressions (Zimmerman, 1980; Park and Wang, 1994). In the present experiment, the tidal residual currents intensify to the right of the bank, where they generate a northeastward-flowing jet. The tidally driven anticyclone is accompanied by smaller subgyres near the northern and southern tips of the mouth and near Cape Dos Bahías and on Camarones Bay (Figure 2a).

The experiment forced with both tides and winds is similar to the wind-driven case, but the anticyclonic gyre expands toward the north and toward the outer shelf. This experiment also shows the development of an additional recirculation cell with intense residual jets over South Bank. The general circulation structure of this experiment is similar to previous barotropic simulations of the Patagonian Shelf (Palma et al., 2004a; Tonini et al., 2006).

STRAT

This experiment considers the impact of density stratification on the gulf circulation.

Time Mean Circulation

The differences between NONSTRAT and STRAT demonstrate the impact of intrusions of the Patagonia Current and atmospheric heat and freshwater fluxes on the GSJ circulation. The large anticyclonic gyre shown in the wind and tide version of NONSTRAT shrinks considerably and is confined to the southernmost edge of the gulf, while the northernmost cyclonic gyre expands to encompass most of the gulf (Figure 2c,d). The STRAT circulation is particularly influenced by the intrusion of the Patagonia Current. Approximately one-third of the volume transport of this current is entrained as a loop current that flows along the GSJ coast until ~46°S, where it retroflects and veers offshore. The Patagonia Current intrusion intensifies the recirculation gyre in the southern portion of the domain and contributes to the broad northeastward flow that detrains the gulf's waters onto the open shelf. The STRAT experiment also reveals the development of several recirculation cells, the most prominent of which is an anticyclonic gyre located over South Bank. Smaller anticyclonic gyres are also observed over a small-scale bank located in the central northern half of the GSJ, in coastal regions of the southern half, and in Camarones Bay (on the northern shelf). The impact of density stratification is reflected not only in the intensities of the flows but also in their directions (Figure 2c,d).

Substantial portions of the NONSTRAT/STRAT differences are associated with the density gradients generated by the Patagonia Current's intrusion and the atmospheric heat and freshwater fluxes. These differences are particularly large because the STRAT time mean circulation is dominated by the patterns established during the austral summer, when density stratification peaks and circulation is more intense (Figure 3a). The vertical structure of the summer circulation is illustrated in three horizontal cross-sections representing surface, intermediate, and bottom layers (Figure 4). At the surface, there is a broad northeastward flow that is largely driven by Ekman dynamics. The thermohaline structure of this layer highlights the impact of the cool and fresh waters of the Patagonia Current on the local thermohaline structure (Figure 4a,d). Two temperature maxima are observed near coastal regions, one in the south (16°C) and the other in the north (>17°C). The two thermal fronts generated by the model are in agreement with satellite observations (Glembocki et al., 2015). The strongest front is located at the mouth of the gulf and intensifies north of 46.5°S. The weaker front, located near the southern coast, is generated by the intrusion of cold Patagonia Current waters. Glembocki et al. (2015) also reported a third thermal front that is not reproduced by our model. The influence of the Patagonia Current on the gulf's thermohaline structure is more evident in the subsurface layer, which shows the penetration of a cool and fresh tongue of water that is subsequently recirculated in the interior of the gyre (Figure 4b–e). This intrusion divides the gulf into a cool and relatively fresh southern sub-basin and a warm and saltier one. As the waters of the Patagonia Current spread into the gulf, mixing and atmospheric fluxes erode their original thermohaline characteristics.

Circulation in the bottom layer of the model is more complex than in the surface due to its stronger dependence on bathymetric features, although it is still easy to recognize the imprint of the upper circulation (Figure 4c–f). In the interior of the basin, for example, the bottom circulation reflects the cyclonic and anticyclonic gyres of the upper layers. The largest differences between surface and deeper layers are observed in the coastal region, where the intense cyclonic coastal current flowing in the upper layers is replaced by a weak anticyclonic flow at depth. The convergences and divergences of the velocity field in the deep layer reflect coastal upwelling and downwelling processes. Bottom currents, for example, are directed toward the coast at the tip of Cape Dos Bahías and at the southwestern coast of the basin. These coastal convergences promote upwelling of colder water in the latter but not in the former (Figure 4a). The differences are likely related to differences in the topographic slopes of the two locations. The bottom circulation is also influenced by the penetration of fresher waters of the Patagonia Current, which after passing Cape Tres Puntas generate a spiral of fresher waters along the southern margin of the gulf (Figure 4f). A tongue of low-salinity waters along the gulf's mouth marks the pathway of the remaining portion of the Patagonia Current (Figure 4f).

Cross sections of model variables along the mouth of the GSJ allow identification of the preferential sites of mass exchange with the open shelf. The temperature cross section shows three distinct regions: a southern region, which is well mixed and relatively warm; a northern region (north of ~46.3°S), which is strongly stratified and includes a relatively deep (20 m) mixed layer; and a central region, which is weakly stratified and exhibits colder temperatures than the southern sector (Figure 5a). The salinity cross section shows a relatively fresh and well-mixed region in the south and a nearly homogeneous structure in the north (Figure 5b). The large velocities near the southern and northern boundaries represent interior outflows, except those attached to a thin boundary layer near the southern coast, where there is an inflow (Figure 5c).

The southern and northern outflowing jets display contrasting spatial structures. The southern jet, which reflects the dominant barotropic structure of the anticyclonic gyre, has a restricted connection to the shelf. The northern jet, which has a well-defined baroclinic structure, is the main conduit for outflow of the interior waters to the exterior shelf. There is also an outflow of gulf waters in a thin surface Ekman layer. The compensating inflow is concentrated in several velocity cores at subsurface layers (~10–30 m; Figure 5c). The southern and more intense of these cores feeds the loop current (Figure 4b). The weakest core is generated by the meandering path of the loop current to the north of 46°S. There is also an additional inflow of shelf waters near the bottom layer in the northern half of the mouth, particularly below the outflowing coastal jet.

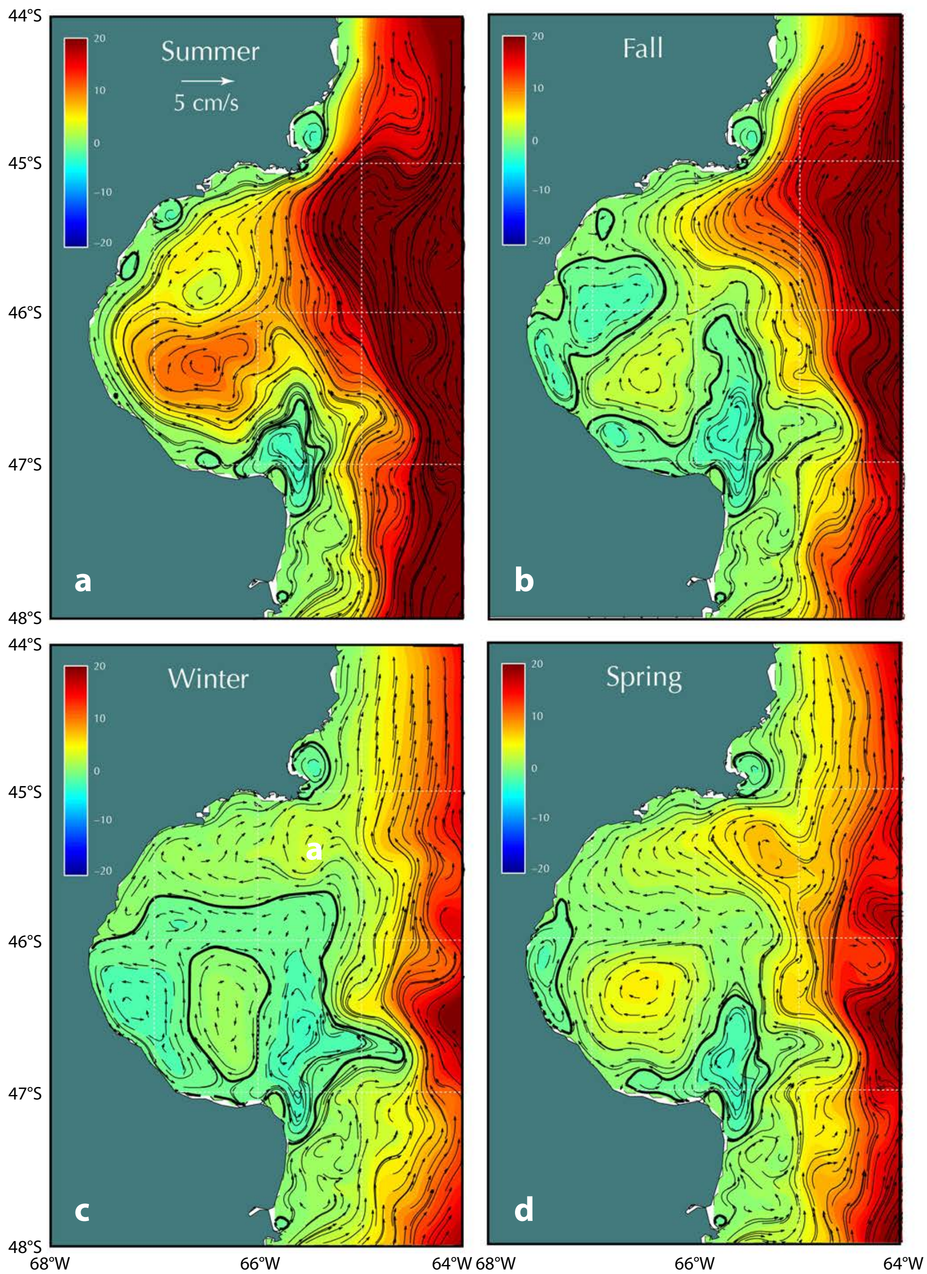

FIGURE 3. Seasonal evolution of the stream function (colors in cSv) and residual (30-day average) depth-mean velocity vectors from STRAT. (a) Summer. (b) Fall. (c) Winter. (d) Spring. Thick black lines indicate the zero contour.

Seasonal Variability

The seasonal variability of the GSJ circulation is dominated by two distinct circulation structures that reach their maximum expressions during the summer and winter seasons (Figure 3a,c). These patterns are bridged by transition circulation patterns during fall and spring (Figure 3b,d). During summer the cyclonic circulation reaches its maximum intensity and extension (Figure 3a). On the one hand, the strengthening of vertical density gradients favors the tidally induced generation of baroclinic pressure gradients that enhance cyclonic motions. On the other hand, this strengthening ameliorates the influence of bottom topography, thus inhibiting the wind-forcing tendency to develop the southern anticyclonic gyre (e.g., Figure 2c). During summer, the mass exchanges between the gulf and the shelf reach their maxima (Figure 5d). The southern loop and cyclonic coastal currents disappear toward the fall when there is a marked weakening of the cyclonic circulation and an expansion of the northern anticyclonic gyre on the northwest coast of the gulf (Figure 3b). The southern recirculating cyclonic gyre wanes while the anticyclone located over South Bank expands meridionally, displacing the core of the loop current to the north (Figure 3b). During this season, mass exchanges between the gulf and the open shelf are largely restricted to the northern portion of the gulf (Figure 5d). Strong thermal convection during winter leads to homogenization of the water column, thus allowing the stronger westerly winds to generate two anticyclonic subgyres (Figure 3c). The larger, located in the southwestern region, is characterized by an intense southward flowing coastal current. The smaller extends along South Bank, thus reflecting the contribution of tidal residual currents to the circulation in this region (Figure 2b). During winter, the inner shelf circulation weakens and the core of the Patagonia Current moves offshore; combined with the partial blocking of the mouth by the elongated anticyclonic gyre, this movement reduces the exchange between the gulf

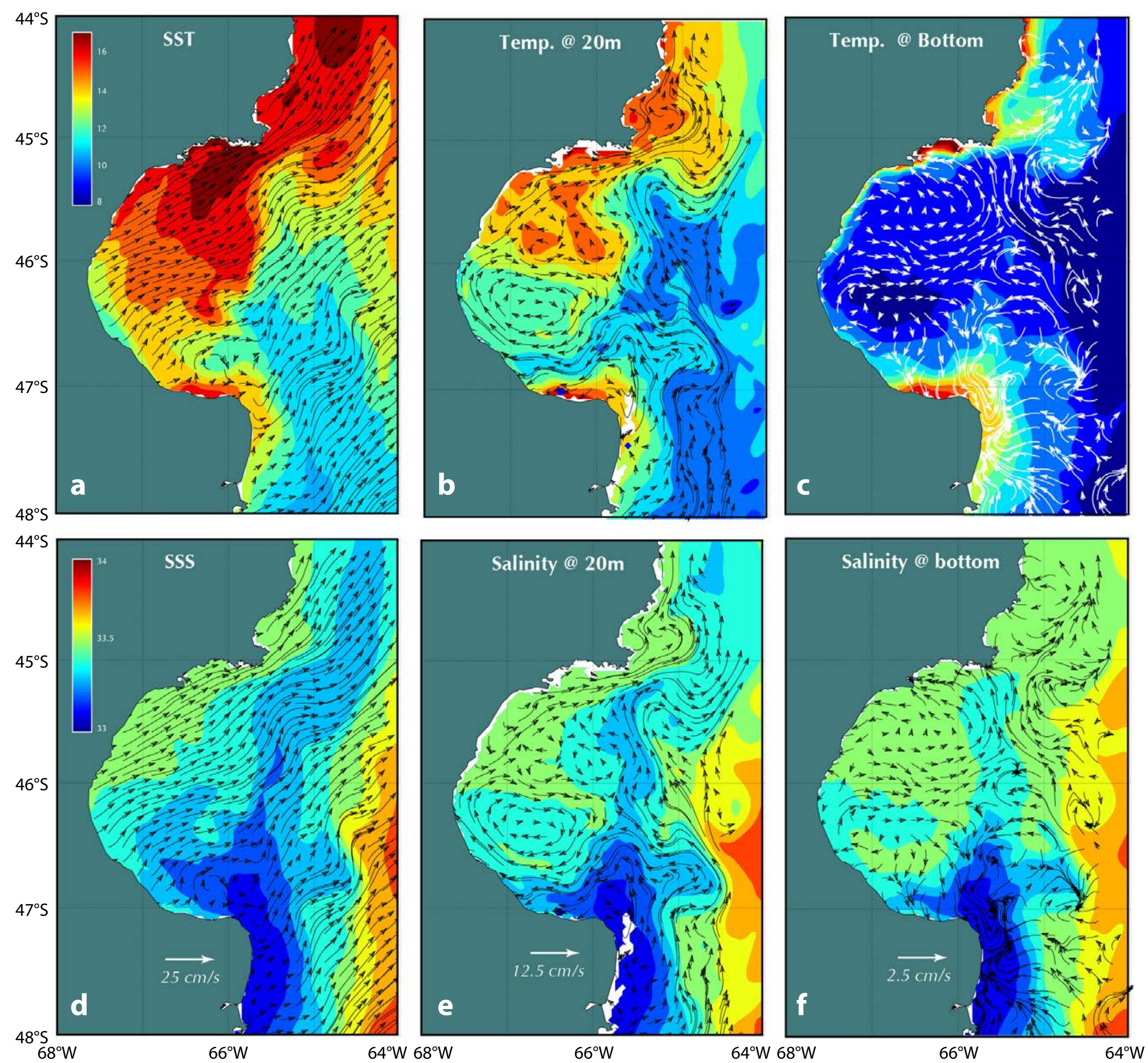

FIGURE 4. Summer mean temperature and salinity fields (colors) and velocity vectors at three different levels in the water column: surface (left panels), subsurface (20 m depth, middle panels) and bottom layer (right panels) from the STRAT experiment.

and the shelf (Figure 5d). During this season, GSJ/shelf mass exchanges are confined to a small sector of the northern region. During the early months of spring, the wind weakens and the increasing heat flux from the atmosphere starts to restratify the gulf's waters. As a result, the southern cyclonic gyre begins to spin up while the southwestern anticyclonic gyre shrinks in size. By late spring, the increased interaction between tides and stratification intensifies the cyclonic gyre and generates a weak loop current in the southern region (Figure 3f). In the northern region, the cyclonic circulation strengthens, boosted by penetration of the Patagonia Current. During spring, the mass exchanges between the gulf and the shelf are largely confined to the northern region, although there is also a recognizable inflow south of 46°S (Figure 5d). As the season progresses, the cyclonic circulation extends to the coast of the southern portion of the gulf, and in January, the summer circulation pattern emerges again.

DISCUSSION

The strong seasonal changes of the GSJ circulation renders any consideration of the mean circulation meaningless. Seasonal variations in GSJ circulation are characterized by two distinct circulation modes, which are shown in our title page image. During summer, a gulf-wide cyclonic coastal current system bounds a cyclonic gyre in the south and a weak anticyclonic gyre in the north. The coastal current is reinforced by the intrusion of a branch of the Patagonia Current, which loops around the gulf. During winter, the combined action of deep convection and wind forcing generate a large anticyclonic gyre in the southwestern sector of the gulf with intense southward subsurface coastal flow. During this season, the coastal current weakens considerably and the recirculating cyclonic gyre in the southern region nearly disappears as the baroclinic tendency within the model domain is overwhelmed by convection and increased wind forcing. The mass exchanges between the GSJ and the shelf peak during summer and are at a minimum in winter. At that time, the weak exchanges between the GSJ and the Patagonian Shelf are confined to the northern region, where the Patagonian Current intrudes in an abrupt cyclonic loop that reaches the coast. Fall and spring represent transition periods (Figure 3). In fall, there is spin-down of the cyclonic circulation and a steady increase of the anticyclonic coastal gyres. During spring, the cyclonic circulation spins up, starting with the southern cyclonic gyre and the northwest coastal current, while the anticyclonic gyre shrinks in size. Superimposed on this circulation pattern, there is an anticyclonic gyre over the South Bank that persists all year.

There are few direct current observations in the GSJ to validate model results. However, patterns similar to those described herein have been reported in other gulfs. Xue et al. (2000), for example, described a summer intensification of a coastal cyclonic circulation in the Gulf of Maine. They attribute this behavior to

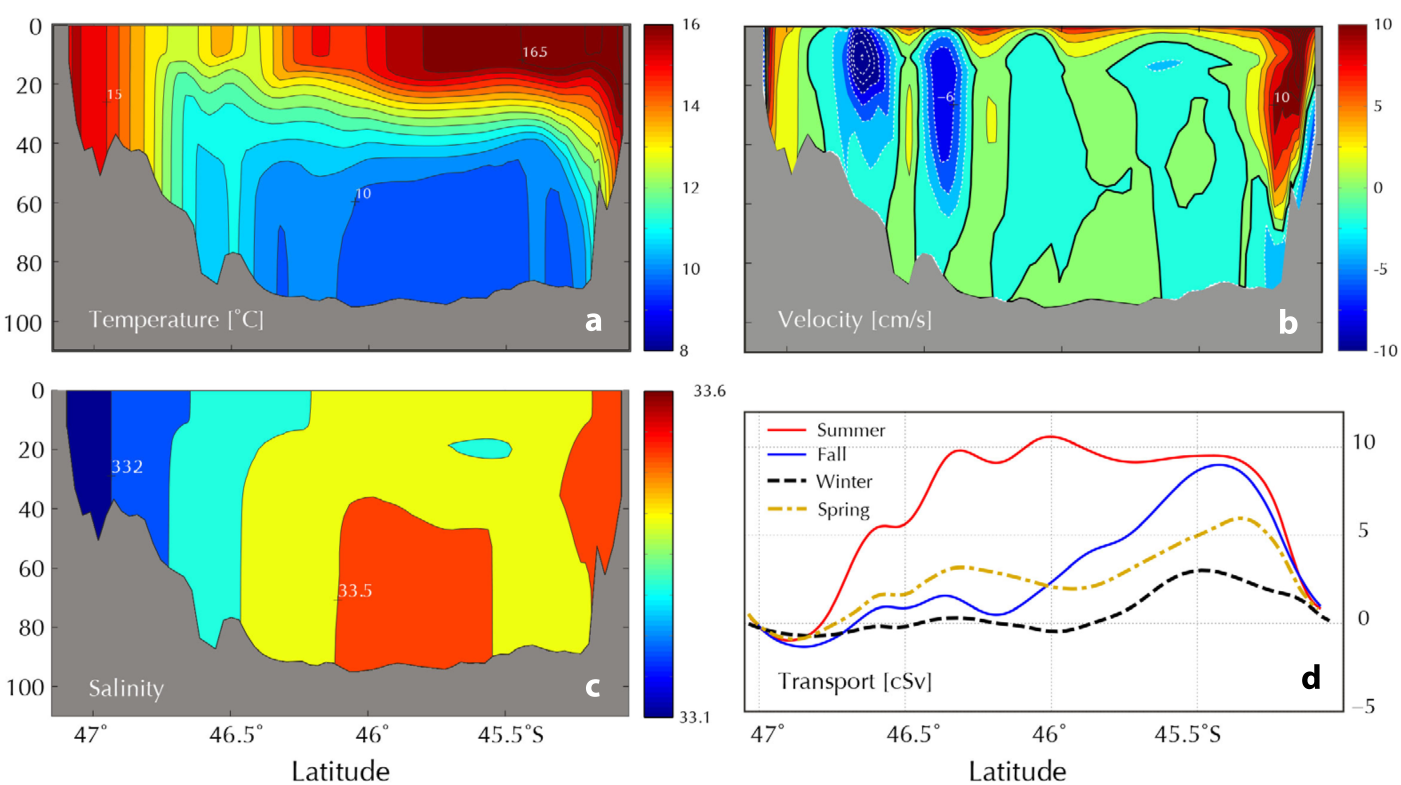

FIGURE 5. Summer mean temperature (a), salinity (b) and cross-shore velocity (c) at a meridional section crossing the gulf's mouth from the STRAT experiment. (d) Water exchange (in cSv) through the mouth in different months. Positive (negative) slope indicates inshore (offshore) transport.

differential heating of coastal (warmer) and offshore (cooler) areas of the gulf and its interaction with intense tidal mixing. Summer cyclonic recirculating patterns like the one observed over the GSJ Central Basin are also expected in small and deep sub-basins if a cold-water pool produced by winter cooling is isolated by tidal mixing during the start of stratification (Hill, 1996). Similar cyclonic recirculating patterns associated with dense bottom lenses have been observed and modeled in the Gulf of California (Lavin et al., 1997), the Yellow Sea (Hu et al., 1991), the Irish Sea (Hill et al., 1997), and the Argentinean North Patagonian Gulfs (Tonini et al., 2013). While mostly barotropic in nature, the main anticyclonic gyres are driven by different forcing mechanisms. The southeastern gyre is driven by tidal rectification over the South Bank, and the southwestern gyre is generated by westerly winds acting on the particular geomorphology of the gulf. These results are consistent with similar barotropic models of the Patagonian Shelf gulfs (Palma et al., 2004a; Tonini et al., 2006; Tonini and Palma, 2017).

In summary, the model results suggest that seasonal variations of the GSJ circulation are partly driven by local atmospheric forcing and partly by tidal forcing and intrusions of the Patagonia Current. The overall impact of these distinct forcing mechanisms is regulated by the bottom topography. During summer, the circulation is mainly controlled by the interaction between tides and stratification, and during winter by wind forcing.

REFERENCES

Barnier, B. 1998. Forcing the ocean. Pp. 45–80 in *Ocean Modelling and Parameterization*. E.P. Chassingnet and J. Verron, eds, Kluwer Academic Publishers, The Netherlands.

Bogazzi, E., A. Baldoni, A. Rivas, P. Martos, R. Reta, J.M. Orensanz, M. Lasta, P. Dell'Arciprete, and F. Werner. 2005. Spatial correspondence between areas of concentration of Patagonian scallop (*Zygochlamys patagonica*) and frontal systems in the southwestern Atlantic. *Fisheries and Oceanography* 14:359–376, https://doi.org/10.1111/j.1365-2419.2005.00340.x.

Brandhorst,W., and J.P. Castello. 1971. *Evaluación de los recursos de anchoita (Engraulis Anchoita) frente a la Argentina y Uruguay: Parte I. Las condiciones oceanográficas, sinopsis del conocimiento actual sobre la anchoita y el plan para su evaluación*. Proy. Des. Pesq. Ser., FAO, 29, 63 pp.

Combes, V., and R.P. Matano. 2014. A two-way nested simulation of the oceanic circulation in the Southwestern Atlantic. *Journal of Geophysical Research Oceans* 119:731–756, https://doi.org/10.1002/2013JC009498.

Conkright, M.E., R.A. Locarnini, H.E. Garcia, T.D. OBrien, T.P. Boyer, C. Stephens, and J.I. Antonov. 2002. *World Ocean Atlas 2001: Objective Analyses, Data Statistics, and Figures*. National Oceanographic Data Center, Silver Spring, MD, CD-ROM Documentation, 17 pp.

Costanza, R., R. d'Arge, R. de Groot, S. Farber, M. Grasso, B. Hannon, K. Limburg, S. Naeem, R.V. O'Neill, J. Paruelo, and others. 1997. The value of the world's ecosystem services and natural capital. *Nature* 387:253–280, https://doi.org/10.1038/387253a0.

Debreu, L., P. Marchesiello, P. Penven, and G. Cambon. 2012. Two-way nesting in split-explicit ocean models: Algorithms, implementation and validation. *Ocean Modelling* 49:1–21, https://doi.org/10.1016/j.ocemod.2012.03.003.

Egbert, G.D., A.F. Bennett, and M.G. Foreman. 1994. TOPEX/Poseidon tides estimated using a global inverse model. *Journal of Geophysical Research* 99:24,821–24,852, https://doi.org/10.1029/94JC01894.

Glembocki, N.G., G.N. Williams, M.E. Góngora, D.A. Gagliardini, and J.M. Orensanz. 2015. Synoptic oceanography of San Jorge Gulf (Argentina): A template for Patagonian red shrimp (*Pleoticus muelleri*) spatial dynamics. *Journal of Sea Research* 95:22–35, https://doi.org/10.1016/j.seares.2014.10.011.

Glorioso, P.D., and R.A. Flather. 1995. A barotropic model of the currents off SE South America. *Journal of Geophysical Research* 100:13,427–13,440, https://doi.org/10.1029/95JC00942.

Hill, A.E. 1996. Spin-down and the dynamics of dense pool gyres in shallow seas. *Journal of Marine Research* 54(16):471–486, https://doi.org/10.1357/0022240963213538.

Hill, A.E., J. Brown, and L. Fernand. 1997. The summer gyre in the Western Irish Sea: Shelf sea paradigms and management implications. *Estuarine, Coastal and Shelf Science* 44A:83–95, https://doi.org/10.1016/S0272-7714(97)80010-8.

Hu, D., M. Cui, Y. Li, and T. Qu. 1991. On the Yellow Sea cold water mass related circulation. *Yellow Sea Research* 4:79–88.

Krock, B., C.M. Borel, F. Barrera, U. Tillmann, E. Fabro, G.O. Almandoz, M. Ferrairo, J.E. Garzón Cardona, B.P. Koch, C. Alonso, and others. 2015. Analysis of the hydrographic conditions and cyst beds in the San Jorge Gulf, Argentina, that favor dinoflagellate population development including toxigenic species and their toxins. *Journal of Marine Systems* 148:86–100, https://doi.org/10.1016/j.jmarsys.2015.01.006.

Large, W., J. McWilliams, and S. Doney. 1994. Oceanic vertical mixing: A review and a model with a nonlocal boundary-layer parameterization. *Review of Geophysics* 32(4):363–403, https://doi.org/10.1029/94RG01872.

Lavin, M.F., R. Durazo, E. Palacios, M.L. Argote, and L. Carrillo.1997. Lagrangian observations of the circulation in the Northern Gulf of California. *Journal of Physical Oceanography* 27:2,298–2,305, https://doi.org/10.1175/1520-0485(1997)027<2298:LOOTCI>2.0.CO;2.

Marchesiello, P., J.C. McWilliams, and A. Shchepetkin. 2001. Open boundary conditions for long-term integration of regional oceanic models. *Ocean Modelling* 3:1–20, https://doi.org/10.1016/S1463-5003(00)00013-5.

Palma, E.D., and R.P. Matano. 2012. A numerical study of the Magellan plume. *Journal of Geophysical Research* 117, C05041, https://doi.org/10.1029/2011JC007750.

Palma, E.D., R.P. Matano, and A.R. Piola. 2004a. A numerical study of the Southwestern Atlantic Shelf circulation: Barotropic response to tidal and wind forcing. *Journal of Geophysical Research Oceans* 109, C08014, https://doi.org/10.1029/2004JC002315.

Palma, E.D., R.P. Matano, and A.R. Piola. 2008. A numerical study of the Southwestern Atlantic Shelf circulation: Stratified ocean response to local and offshore forcing. *Journal of Geophysical Research* 113, C11010, https://doi.org/10.1029/2007JC004720.

Palma, E.D., R.P. Matano, A.R. Piola, and L. Sitz. 2004b. A comparison of the circulation patterns over the Southwestern Atlantic driven by different wind stress climatologies. *Geophysical Research Letters* 31, L24303, https://doi.org/10.1029/2004GL021068.

Park, M.J., and D.P. Wang. 1994. Tidal vorticity over isolated topographic features. *Continental Shelf Research* 14(13/14):1,583–1,599, https://doi.org/10.1016/0278-4343(94)90091-4.

Silwan, C.A. 2001. Geology of the Golfo San Jorge Basin, Argentina. *Journal of Iberian Geology* 27:123–157.

Tonini, M.H., and E.D. Palma. 2017. Tidal dynamics on the North Patagonian Argentinean Gulfs. *Estuarine, Coastal and Shelf Science* 65:97–110, https://doi.org/10.1016/j.ecss.2017.02.026.

Tonini, M.H., E.D. Palma, and A.R. Piola. 2013. A numerical study of gyres, thermal fronts and seasonal circulation in austral semi-enclosed gulfs. *Continental Shelf Research* 65:97–110, https://doi.org/10.1016/j.csr.2013.06.011.

Tonini, M.H., E.D. Palma, and A.L. Rivas. 2006. Modelo de alta resolución de los golfos norpatagónicos. *Mecánica Computacional* XXV:1,441–1,460.

Xue, H., F. Chai, and N.R. Pettigrew. 2000. A model study of the seasonal circulation in the Gulf of Maine. *Journal of Physical Oceanography* 30:1,111–1,135, https://doi.org/10.1175/1520-0485(2000)030<1111:AMSOTS>2.0.CO;2.

Zimmerman, J.T.F. 1980. Vorticity transfer by tidal currents over an irregular topography. *Journal of Marine Research* 38:601–630.

ACKNOWLEDGMENTS

R. Matano acknowledges NASA support through grant NNX17AH20G and the National Science Foundation through grants OCE-1357530 and OCE-1559550. E.D. Palma acknowledges financial support from Agencia Nacional de Promoción Científica y Tecnológica (grant PICT16-0557) and Universidad Nacional del Sur (grant 24F066), Argentina.

AUTHORS

Ricardo P. Matano (rmatano@coas.oregonstate.edu) is Professor, College of Earth, Ocean, and Atmospheric Sciences, Oregon State University, Corvallis, OR, USA. **Elbio D. Palma** is Professor, Departamento de Física, Universidad Nacional del Sur, and Researcher, Instituto Argentino de Oceanografía, Consejo Nacional de Investigaciones Científicas y Técnicas, Bahia Blanca, Argentina.

ARTICLE CITATION

Matano, R.P., and E.D. Palma. 2018. Seasonal variability of the oceanic circulation in the Gulf of San Jorge, Argentina. *Oceanography* 31(4):16–24, https://doi.org/10.5670/oceanog.2018.402.